Scalable Distributed Optimization Combining Conic Projection and Linear Programming for Energy Community Scheduling

Mohammad Dolatabadi, Alberto Borghetti, and Pierluigi Siano

***Abstract*—In this paper, a new method to address the scheduling problem of a renewable energy community while considering network constraints and users' privacy preservation is proposed. The method decouples the optimization solution into two interacting procedures: conic projection (CP) and linear programming (LP) optimization. A new optimal CP method is proposed based on local computations and on the calculation of the roots of a fourth-order polynomial for which a closed-form solution is known. Computational tests conducted on both 14-bus and 84-bus distribution networks demonstrate the effectiveness of the proposed method in obtaining the same quality of solutions compared with that by a centralized solver. The proposed method is scalable and has features that can be implemented on microcontrollers since both LP and CP procedures require only simple matrix-vector multiplications.**

***Index Terms*—Accelerated gradient method, battery storage system, conic projection, energy community, energy scheduling, linear programming, renewable resource.**

I. Introduction

To guarantee more sustainable and reasonable access to energy, the recent evolution of the regulatory frameworks in Europe and elsewhere has promoted the centrality of prosumers and the diffusion of renewable energy sources, distributed generation, and energy storage systems [1].

Because of improved metering and other information- and communication-technology-based infrastructures, a new paradigm for managing smart grids has garnered interest. This new paradigm involves establishing energy communities based on an aggregation of prosumers, allowing direct power exchanges. Because electricity exchanges contribute to the improved exploitation of renewable energy resources and allow the provision of power flexibilities at reduced costs, prosumers can benefit from their participation in an energy community. The participation of energy communities in ancillary service markets (e.g., [2] and references therein) is another interesting aspect worthy of study.

Recent research works in the field of energy communities have focused on energy exchanges and pricing models [3]-[10] by using different methods such as game theory [3], [9], decentralized bilateral trading [4], [5], and market models (e.g., [6]) for distribution networks. In [7], a sensitivity analysis is used to assess the effects of transactions on the network constraints. An energy-trading method is proposed in [8] to mitigate the peak demand by incentivizing prosumers to conduct energy exchanges. A game-theoretic method with heterogeneous prosumers who trade energy for virtual microgrids is proposed in [9]. In [10], an energy block contract market is solved by using a privacy-preserving distributed algorithm that allows users to trade services in a flexible manner.

Power losses and/or technical constraints in the network are often neglected in studies on energy exchange. By neglecting power losses, the power balance conditions are not precisely evaluated [11]. In this regard, different methods have been proposed to address this issue. In [12], power losses are allocated to each bus of a microgrid, and battery storage units are discharged to compensate for the power losses. A market with energy exchanges is considered in [13], and a second-order cone programming (SOCP) formulation is devised for the allocation of power losses. The two considered configurations couple peer-to-peer (P2P) interactions with distribution network operations using a centralized or P2P procedure. In the second case, the utility and the P2P platform are operated separately, and the coordination between them is achieved by an iterative procedure. Network fees and power losses are considered in [11], whereas a power transfer distribution factor is used in [3] and [4] to evaluate the effects of transactions on power flow constraints. The effects of the low-voltage networks on local markets are evaluated in [14]. Electrical distances between prosumers and the shortest path algorithm are used in [15]. An estimation method for the allocation of power losses to each transaction is used in the alternating direction method of multipliers (ADMM)-based method presented in [16] and extended in [17]

Manuscript received: November 29, 2022; revised: February 21, 2023; accepted: April 11, 2023. Date of CrossCheck: April 11, 2023. Date of online publication: May 25, 2023.

M. Dolatabadi is with the Department of Mathematics, Vali-e-Asr University of Rafsanjan, Rafsanjan 77188-97111, Iran (e-mail: author1@lamar. colostate. edu).

A. Borghetti is with the Department of Electrical, Electronic, and Information Engineering, University of Bologna, Bologna, Italy (e-mail: alberto. borghetti@unibo.it).

P. Siano (corresponding author) is with the Department of Management & Innovation Systems, University of Salerno, Salerno, Italy, and he is also with the Department of Electrical and Electronic Engineering Science, University of Johannesburg, Johannesburg 2006, South Africa (e-mail: psiano@unisa.it).

DOI: 10.35833/MPCE.2022.000783

to consider the link between day-ahead and intraday scheduling (a topic also dealt with in [18]). In [19], a mixed-integer centralized model of a local energy community (LEC) is proposed that adopts the classical SOCP convex relaxation of the optimal power flow problem (e.g., [20], [21] and references therein).

P2P methods are particularly attractive because of the specific characteristics of energy communities in which multiple independent prosumers collaborate to reach a common objective, where the primary objective is the reduction of energy procurement costs.

In [22], a P2P active power management framework based on a multi-agent distribution system is described in which only the operational constraints of the agents' resources and the supply-demand balance constraints are considered. A P2P management model is adopted to facilitate the independent optimization of the agents' operational plans. In [23], Nash bargaining theory is used to formulate a P2P transactive energy trading problem that is decomposed into an optimal power flow (OPF) problem and a payment bargaining problem. ADMM is adopted to solve distributed optimization in a privacy-preserving manner. In [24], a P2P platform is presented that can minimize the costs associated with battery depreciation and power losses. In this case, distributed optimization is solved by using the ADMM while considering network constraints. In [25], a P2P electricity trading framework based on the generalized fast dual ascent method is proposed. Network constraints are considered in the proposed model through a voltage and loss sensitivity method. In [26], the proposed distribution system operator-prosumer scheduling framework is based on Nash bargaining. The problem is decomposed into two subproblems and solved in a distributed manner using ADMM. In [27], the proposed optimization is based on the virtual model of self-consumption, where the energy balance within the community is accomplished by considering the energy exchanges assessed at each point of delivery. This results in scalable and privacy-preserving real-time distributed parallel optimization for the participation of an energy community in the ancillary service market.

It is assumed that the LEC is managed by an energy community manager that performs the scheduling optimization aiming at minimizing the costs related to the energy consumption in the community or maximizing the revenues when the community globally exports power. Prosumers can be endowed with local generation, photovoltaic (PV) units, and/or battery systems. Cost minimization is achieved by favoring direct energy exchanges among prosumers while optimizing the use of internal energy resources.

Depending on their needs and the choices of the energy community manager, prosumers can consume energy from the external energy provider (here, for simplicity, this corresponds to the utility grid) and can use the electrical energy produced by their PV plant by consuming it themselves. Moreover, prosumers can share energy with other prosumers or store it in their local batteries.

The fair prices of the energy exchanges are automatically computed by the optimization procedure while considering both the time and location of the involved prosumers. The prices are based on the calculation of the dual variables of the balancing constraints relevant to the energy exchanges in the optimization model.

This paper focuses on a deterministic model, and the test results are presented for a typical time horizon of 24 hours. To consider the uncertainties associated with PV production and load forecasting, the procedure has the computational characteristics necessary for inclusion in a scenario-based stochastic method and for application in rolling horizon intraday procedures such as those described in [27].

Unlike in the centralized model of [19], the proposed method does not use binary variables, and the set of constraints is decoupled into a conic projection (CP) procedure plus a linear programming (LP) problem, both of which are solved in a decentralized privacy-preserving manner.

To solve the SOCP optimization, a specific CP procedure is applied locally so that the user's information is not disclosed. In contrast with, e.g., [28], the P2P exchanges are not virtual, and network constraints and power losses are evaluated.

To better highlight the innovative contribution of the proposed method, Table I compares some key features of the methods already presented in the literature.

The comparison shows that only a few papers present a distributed optimization considering conic constraints, power losses, and the privacy of prosumers [6], [23], [26], which are the main characteristics of the proposed method. In [6], the nonconvex constraints for Distflow equations are approximated by using an implicit function instead of the SOCP formulation. In [23] and [26], the SOCP formulation is adopted and embedded in sequential ADMM procedures. As regards the privacy issue, in [6] and [23], the respect for user privacy is assumed because the optimization is performed in a fully distributed manner with ADMM, while in [26], the privacy is preserved by using consensus-based ADMM.

The proposed method has the following original characteristics and specific advantages.

1) A new optimal CP method is proposed based on local computations. It is presented in detail in the Appendix A and is based on the calculation of the roots of a fourth-order polynomial for which a closed-form solution is known.

2) A new method for users' privacy preservation based on data aggregation is proposed that decouples the optimization solution into two interacting procedures, namely, CP and LP optimization. In contrast to the previous methods, the implemented procedure is based on parallel matrix-vector multiplications which allow the implementation of a parallel procedure. After the penalized LP is solved, an individual and independent CP procedure is conducted for each user in a private and parallel manner. If the summation of infeasibility for the conic constraints remains greater than the required accuracy, another penalized LP is obtained. These two interacting LP and CP procedures continue until convergence.

3) The prices of the internal P2P transactions can be evaluated by using the dual variables associated with the power equilibrium constraints.

TABLE I
COMPARISONS WITH PREVIOUS METHODS

Ref.	Conic constraint	Power loss of prosumer	Privacy	Method
[3]	n	n	No	Stackelberg game
[4]	n	n	Yes	Decentralized P2P energy trading scheme
[5]	n	y	No	Iterative peer matching process
[6]	y	y	Yes	ADMM
[7]	y	y	No	Methodology based on sensitivity analysis
[8]	n	n	No	Stackelberg game
[9]	n	n	No	Stackelberg game
[10]	n	y	Yes	Decentralized market clearing mechanism
[12]	n	y	No	Distributed consensus algorithm
[13]	y	y	Yes	Centralized AC OPF and iterative procedure
[14]	y	y	No	Forward/backward sweep method with power summation
[15]	n	y	Yes	Two market mechanisms for P2P energy trading driven by electrical distance
[16]	y	y	No	ADMM
[17]	y	y	No	ADMM
[18]	n	n	Yes	Decentralized sequential decision making model
[19]	y	y	No	Mixed-integer centralized model
[22]	n	y	Yes	Step-wise transactive distributed control framework
[23]	y	y	Yes	ADMM
[24]	n	y	Yes	ADMM
[25]	n	y	Yes	Fast dual ascent method
[26]	y	y	Yes	ADMM
[28]	n	n	Yes	P2P exchanges based on virtual model of self-consumption
This Paper	y	y	Yes	LP-based optimization

Note: y means that it is included in the method; n means that it is not included.

4) The proposed method can be easily implemented without using any commercial or open-source solver.

In previous studies, the ADMM is employed to solve the distributed optimization by using off-the-shelf solvers such as Gurobi in [6] and [23], CPLEX in [24], and MOSEK in [26].

As mentioned, the proposed alternating projection method consists of the two LP and CP procedures. The solution to LP is based on matrix-vector multiplications. At each iteration, the only calculation performed by each prosumer is matrix-vector multiplication plus local CP. It is worth noting that without the CP part, the LP part exhibits a convergence rate of $O(1/k^2)$, while the ADMM used in [6], [23], [26] exhibits a convergence rate of $O(1/k)$ [28], [29].

The remainder of the paper is organized as follows. The proposed model is described in Section II. Section III presents the solution procedure. Section IV presents the test results, and Section V gives conclusions.

II. PROPOSED MODEL

As in [19], the proposed model represents the internal network of the LEC as a combination of lines connected to each other with a radial configuration and balanced for a single-phase representation. At the end of each line, a prosumer is connected.

Including the feeding line, each prosumer is defined by two connection points, herein denoted as the input and output sides. The input side is connected to the slack bus (i.e., the medium-voltage (MV) secondary side of the substation transformer) or to the output side of the upstream branch. The output side is connected to the input side of the downstream branch or it is not connected in the case of the terminal branches of the system.

In the model, the set of all prosumers is denoted by Ω (with index i). For each prosumer i and each time interval t (under duration Δt) of the considered optimization horizon T, $v_{\text{in}\,i,t}$ and $v_{\text{out}\,i,t}$ denote the root mean square (RMS) values of the voltages at the input and output terminals, respectively; $u_{i,t}$ denotes the square RMS value of the current of the feeding branch (the charging current is neglected); $P_{\text{in}\,i,t}$ and $P_{\text{out}\,i,t}$ denote the input and output active power flows, respectively; $Q_{\text{in}\,i,t}$ and $Q_{\text{out}\,i,t}$ denote the input and output reactive power flows, respectively; and r_i and x_i denote the line resistance and reactance, respectively.

The prosumer model includes a local load, generating unit, and battery energy storage (BES). $P_{\text{l}\,i,t}$ and $Q_{\text{l}\,i,t}$ are the active and reactive power load consumptions, respectively; $P_{\text{g}\,i,t}$ and $Q_{\text{g}\,i,t}$ are the active and reactive power generation outputs, respectively; $P_{\text{BES}\,i,t}$ is the BES output; and $P_{\text{user}\,i,t}$ and $Q_{\text{user}\,i,t}$ are the total net active and reactive power exchanges, respectively.

The battery model represents the BES energy level ($E_{i,t}$) and charging and discharging battery power losses ($\ell_{\text{charge}\,i,t}$, $\ell_{\text{discharge}\,i,t}$).

Each prosumer may directly perform energy transactions with the utility grid and with other prosumers of the community. $P_{\text{grid}\,i,t}$ is the prosumer's power exchanged with the grid. $P_{\text{buy, grid}\,i,t}$ is the power bought at price $\pi_{\text{buy}\,t}$; $P_{\text{sell, grid}\,i,t}$ is the power sold at price $\pi_{\text{sell}\,t}$; and $P_{\text{LEC}\,i,t}$ is the prosumer's power exchanged with the other prosumers of the community.

In the model and the test results presented in this paper, prices $\pi_{\text{buy}\,t}$ and $\pi_{\text{sell}\,t}$ as well as r_i, x_i, $P_{\text{l}\,i,t}$, $Q_{\text{l}\,i,t}$, $P_{\text{g}\,i,t}$, $Q_{\text{g}\,i,t}$, BES charging and discharging efficiencies ($\eta_{\text{charge}\,i}$ and $\eta_{\text{discharge}\,i}$, respectively), the maximum and minimum limits of $P_{\text{BES}\,i,t}$, $E_{i,t}$, $v_{\text{in}\,i,t}$, $v_{\text{out}\,i,t}$, and the maximum limit of $u_{i,t}$, are considered parameters with predefined values.

To distinguish the power flows due to the transactions between prosumer i and the utility grid from those due to the transactions with other prosumers at each time interval t, the model includes variables $P_{\text{grid, in}\,i,t}$ and $P_{\text{grid, out}\,i,t}$ (i.e., the power flows due to the transactions with the grid at the input and output terminals, respectively) and $P_{\text{LEC, in}\,i,t}$ (i.e., the power flow due to the transactions with other prosumers at the input terminal).

The considered objective minimizes the total community costs due to the transactions with the utility grid:

$$C_{\text{grid}} = \sum_{i \in N} \sum_{t \in T} (\pi_{\text{buy}\,t} P_{\text{buy, grid}\,i,t} - \pi_{\text{sell}\,t} P_{\text{sell, grid}\,i,t}) \Delta t \tag{1}$$

where $P_{\text{buy, grid}\,i,t}$ and $P_{\text{sell, grid}\,i,t}$ are the nonnegative variables. The objective does not include generation costs since we assume here that all the local generation is provided by renewables (e.g., PV panels). When $\pi_{\text{buy}\,t}$ is assumed to be greater than $\pi_{\text{sell}\,t}$, the cost minimization is favored by a balance between the production and consumption in the LEC.

$P_{\text{BES}\,i,t}$ and the trade decisions with the other prosumers of the community are the main decision variables.

Following the typical convention of the Distflow or branch flow model [30], the values of $v_{\text{out}\,i,t}$, $P_{\text{out}\,i,t}$, $Q_{\text{out}\,i,t}$, and $P_{\text{grid, out}\,i,t}$ should be equal to those of $v_{\text{in}\,i+1,t}$, $P_{\text{in}\,i+1,t}$, $Q_{\text{in}\,i+1,t}$, and $P_{\text{grid, in}\,i+1,t}$, respectively, considering i and $i+1$ as the upstream and downstream prosumers, respectively:

$$v_{\text{in}\,i+1,t} - v_{\text{out}\,i,t} = 0 \tag{2}$$

$$P_{\text{in}\,i+1,t} - P_{\text{out}\,i,t} = 0 \tag{3}$$

$$Q_{\text{in}\,i+1,t} - Q_{\text{out}\,i,t} = 0 \tag{4}$$

$$P_{\text{grid, in}\,i+1,t} - P_{\text{grid, out}\,i,t} = 0 \tag{5}$$

In terms of branching for active and reactive power, the equality is replaced by the balancing constraints at the branching node, as in [30].

For the prosumers located at one of the feeder ends, $P_{\text{out}\,i,t}$, $Q_{\text{out}\,i,t}$, and $P_{\text{grid,out}\,i,t}$ are constrained to be 0.

The square RMS voltages at the input terminals of the prosumers connected to the substation should be equal to the known value of the slack bus voltage V_0^2:

$$v_{\text{in}\,k,t} = V_0^2 \quad \forall k \in \Omega_0 \tag{6}$$

where Ω_0 is the set of prosumers connected to the slack bus.

Transactions between the prosumers of the community do not cause any power flow exchange with the grid, i.e.,

$$\sum_{k \in \Omega_0} P_{\text{LEC, in}\,k,t} = 0 \tag{7}$$

For each prosumer i and time interval t, the relationships between $v_{\text{in}\,i,t}$ and $v_{\text{out}\,i,t}$, $P_{\text{in}\,i,t}$ and $P_{\text{out}\,i,t}$, and $Q_{\text{in}\,i,t}$ and $Q_{\text{out}\,i,t}$ are:

$$P_{\text{in}\,i,t} - P_{\text{out}\,i,t} = P_{i,t} \tag{8}$$

$$Q_{\text{in}\,i,t} - Q_{\text{out}\,i,t} = Q_{i,t} \tag{9}$$

$$v_{\text{in}\,i,t} - v_{\text{out}\,i,t} = 2r_i P_{\text{in}\,i,t} + 2x_i Q_{\text{in}\,i,t} - (r_i^2 + x_i^2) u_{i,t} \tag{10}$$

$$P_{\text{in}\,i,t}^2 + Q_{\text{in}\,i,t}^2 \le v_{\text{in}\,i,t} u_{i,t} \tag{11}$$

where nonnegative variable $u_{i,t}$ is constrained to be lower than the square of the maximum branch current limit, nonnegative variables $v_{\text{in}\,i,t}$ and $v_{\text{out}\,i,t}$ are constrained between 0.95^2 p.u. and 1.05^2 p.u., and:

$$P_{i,t} = P_{\text{user}\,i,t} + r_i u_{i,t} \tag{12}$$

$$Q_{i,t} = Q_{\text{user}\,i,t} + x_i u_{i,t} \tag{13}$$

Constraint (11) is the usual rotated second-order cone convex relaxation of the branch flow model. The feasible solution is obtained for an equality condition. The achievement of this condition is checked after the solution, and an iterative procedure is implemented that solves the model with a progressively increased penalization of the branch power losses in the objective function, as described in the final part of this section.

The net power for each prosumer is given by:

$$P_{\text{user}\,i,t} - P_{\text{l}\,i,t} + P_{\text{g}\,i,t} + P_{\text{BES}\,i,t} = 0 \tag{14}$$

$$Q_{\text{user}\,i,t} - Q_{\text{l}\,i,t} + Q_{\text{g}\,i,t} = 0 \tag{15}$$

where $P_{\text{BES}\,i,t}$ is considered positive if supplied by the battery. We assume here that the PV and BES units operate at the unity power factor $Q_{\text{g}\,i,t} = 0$.

The adopted model of the storage units is represented by:

$$P_{\text{BES}\,i,t} - P_{\text{BES}\,i,t}^{+} + P_{\text{BES}\,i,t}^{-} = 0 \tag{16}$$

$$l_{\text{charge}\,i,t} = (1 - \eta_{\text{charge}\,i}) P_{\text{BES}\,i,t}^{-} \tag{17}$$

$$l_{\text{discharge}\,i,t} = \left(\frac{1}{\eta_{\text{discharge}\,i}} - 1 \right) P_{\text{BES}\,i,t}^{+} \tag{18}$$

$$E_{i,t} = E_{i,t-1} - (P_{\text{BES}\,i,t} + l_{\text{charge}\,i,t} + l_{\text{discharge}\,i,t}) \Delta t \tag{19}$$

where $P_{\text{BES}\,i,t}^{+}$ and $P_{\text{BES}\,i,t}^{-}$ are the nonnegative variables constrained by the maximum power limit of the battery.

In the tests, the energy level at the beginning of the first interval and at the end of the optimization horizon are constrained to be equal to the battery rating.

The direct exchanges with the utility grid and those with the other prosumers are described by:

$$P_{i,t} - P_{\text{grid}\,i,t} - P_{\text{LEC}\,i,t} = 0 \tag{20}$$

$$P_{\text{in}\,i,t} - P_{\text{grid, in}\,i,t} - P_{\text{LEC, in}\,i,t} = 0 \tag{21}$$

$$P_{\text{grid}\,i,t} - P_{\text{buy, grid}\,i,t} + P_{\text{sell, grid}\,i,t} = 0 \tag{22}$$

$$P_{\text{grid}\,i,t} - P_{\text{grid, in}\,i,t} + P_{\text{grid, out}\,i,t} = 0 \tag{23}$$

where $P_{\text{buy,grid}\,i,t}$ and $P_{\text{sell,grid}\,i,t}$ are the nonnegative variables.

The modules of the dual values associated with the constraint (20) are used to define the prices of the transactions between the prosumers of the community.

In a feasible solution, (11) is verified as equality. $P_{\text{BES}\,i,t}^{+}$ and $P_{\text{BES}\,i,t}^{-}$ of (16) cannot be both nonzero for the same t and i. Specific checks are included in implementing the model and penalization terms of the line active power losses, and BES losses are added to the objective function.

Moreover, the nonnegative variable $\hat{P}_{\text{LEC}}$ is defined as:

$$\begin{cases} P_{\text{LEC}} - \hat{P}_{\text{LEC}} \le 0 \\ -P_{\text{LEC}} - \hat{P}_{\text{LEC}} \le 0 \end{cases} \tag{24}$$

The reselling of the power from the grid to the other prosumers is avoided by the penalization of $\hat{P}_{\text{LEC}}$ in the objective function, which becomes:

$$OF = \min \left\{ C_{\text{grid}} + \sum_{i \in N} \sum_{t \in T} (\mu_{\text{loss}\,i} r_i u_{i,t} + \mu_{\text{BES}\,i} l_{\text{charge}\,i,t} + \mu_{\text{BES}\,i} l_{\text{discharge}\,i,t} + \mu_{P_{\text{LEC}}} \hat{P}_{\text{LEC}\,i,t}) \Delta t \right\} \tag{25}$$

where $\mu_{\text{loss}\,i}$, $\mu_{\text{BES}\,i}$, and $\mu_{P_{\text{LEC}}}$ are the penalization coefficients

of the line power loss, charging and discharging BES losses, and power exchanges with the other prosumers, respectively. Without penalization term $\mu_{\text{BES}\,i}\ell_{\text{charge}\,i,t}+\mu_{\text{BES}\,i}\ell_{\text{discharge}\,i,t}$, there can be multiple optimal solutions for which battery charging and discharging power are nonzero during the same period t. The penalization term enforces the solver to pick only those solutions for which battery charging and discharging power are both nonzero simultaneously.

When the corresponding feasibility conditions are not met (for all the branches, batteries, and prosumers), new solutions are calculated with the penalization coefficients progressively increased until a feasible one is obtained. For all test results considered in this paper, the weight of the penalization terms of the objective function (25) corresponding to the final feasible solution is negligible with respect to the cost term (1).

In summary, the optimization problem is given by (25), including (1) augmented by the aforementioned penalization terms to guarantee a feasible solution, with constraints (2)-(24), and the lower and upper limits of each variable.

III. Solution Procedure

A. Centralized Method for SOCP

Since the objective function and the constraints described in Section II (excluding (11)) are linear, and because (11) can be re-formulized as the second-order cone $\left\| \begin{matrix} 2P_{\text{in}\,i,t} \\ 2Q_{\text{in}\,i,t} \\ u_{i,t}-v_{\text{in}\,i,t} \end{matrix} \right\|_2^{\text{T}} \le u_{i,t}+v_{\text{in}\,i,t}$, the model can be solved in a centralized manner using a commercial or open-source conic solver such as CPLEX, Gurobi, MOSEK and JuMP in Julia, and MATLAB. In general, the solvers are based on interior point algorithms. In [31], the optimization of a linear objective function over the intersection of an affine space with a convex cone is obtained by using an interior-point method (IPM). In [32], a more numerically stable IPM is proposed using product-form Cholesky factorization.

The typical algorithm implemented in commercial solvers is based on the interior-point method, as described in [31] and [32], for use in the centralized case. The common feature of the interior point method is that a sequence of feasible primal-dual pairs is constructed in a manner in which the gap between primal-dual objective values approaches a desired accuracy. Although these methods are extremely fast, they can have difficulties with large problems, and they do not exploit new hardware accelerators such as GPUs and TPUs. In addition, performing computations in a decentralized manner such that the privacy of the users is respected seems to remain unclear. Accordingly, the proposed method uses gradient information to address large problems in a decentralized privacy-preserving manner.

B. Proposed Decentralized Method

The proposed decentralized method splits the feasible set defined by (2)-(24) into two parts, each of which is easier to handle than the original formulation. Let vector $\boldsymbol{x}$ consist of all decision variables, and denote the feasible set of all constraints (2)-(24) except (11) by $L=\{\boldsymbol{x}|\boldsymbol{Ax}=\boldsymbol{b},\boldsymbol{lb}\le\boldsymbol{x}\le\boldsymbol{ub}\}$ and denote the feasible set of (11) (the second-order cone) by C.

The goal is to optimize (25) over $L\bigcap C$, where L is the set of linear constraints and C is the set of conic constraints. As a result, by excluding (11), we come up with an LP as:

$$\min\{\boldsymbol{c}^{\text{T}}\boldsymbol{x}|\boldsymbol{Ax}=\boldsymbol{b},\boldsymbol{lb}\le\boldsymbol{x}\le\boldsymbol{ub}\} \tag{26}$$

This flow chart of iterative two-stage optimization is illustrated in Fig. 1.

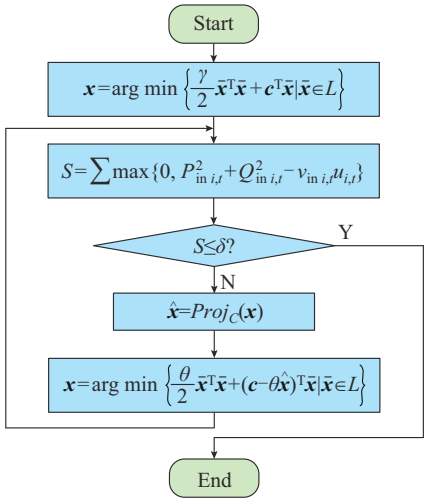

Fig. 1. Flow chart of iterative two-stage optimization.

Step 1: as $\gamma>0$ is a very small constant, $\boldsymbol{x}$ is computed as the optimal solution as (27) by using the procedure presented in Appendix A.

$$\boldsymbol{x}=\arg\min\left\{\frac{\gamma}{2}\bar{\boldsymbol{x}}^{\text{T}}\bar{\boldsymbol{x}}+\boldsymbol{c}^{\text{T}}\bar{\boldsymbol{x}}\,|\,\bar{\boldsymbol{x}}\in L\right\} \tag{27}$$

Step 2: the convergence criteria are checked as to whether $\|\boldsymbol{x}-\hat{\boldsymbol{x}}\|$ and the summation of infeasibilities for linear constraints $\boldsymbol{Ax}=\boldsymbol{b}$ are less than a predefined threshold.

Step 3: $\hat{\boldsymbol{x}}=Proj_C(\boldsymbol{x})$ is the projection of $\boldsymbol{x}$ onto the cone C as defined by (11). If the corresponding entries in solution $\boldsymbol{x}$ (from *Step 1*) do not satisfy (11), and if $|u_{i,t}|>0$, a new solution is obtained by setting $v_{\text{in}\,i,t}=P_{\text{in}\,i,t}^2+Q_{\text{in}\,i,t}^2/u_{i,t}$. If $|u_{i,t}|=0$, the procedure for CP presented in Appendix A is applied.

Step 4: $\boldsymbol{c}^{\text{T}}\bar{\boldsymbol{x}}$ is minimized subject to $\bar{\boldsymbol{x}}\in L$ with the penalization of the distance $\|\bar{\boldsymbol{x}}-\hat{\boldsymbol{x}}\|_2^2$, i. e., $\boldsymbol{c}^{\text{T}}\bar{\boldsymbol{x}}+\frac{\theta}{2}\|\bar{\boldsymbol{x}}-\hat{\boldsymbol{x}}\|_2^2=\frac{\theta}{2}\bar{\boldsymbol{x}}^{\text{T}}\bar{\boldsymbol{x}}+(\boldsymbol{c}-\theta\hat{\boldsymbol{x}})^{\text{T}}\bar{\boldsymbol{x}}+\frac{\theta}{2}\hat{\boldsymbol{x}}^{\text{T}}\hat{\boldsymbol{x}}$, where θ is a penalty term (constant number). As $\hat{\boldsymbol{x}}^{\text{T}}\hat{\boldsymbol{x}}$ is constant, the minimization of $\boldsymbol{c}^{\text{T}}\bar{\boldsymbol{x}}+\frac{\theta}{2}\|\bar{\boldsymbol{x}}-\hat{\boldsymbol{x}}\|_2^2$ is given by:

$$\boldsymbol{x}=\arg\min\left\{\frac{\theta}{2}\bar{\boldsymbol{x}}^{\text{T}}\bar{\boldsymbol{x}}+(\boldsymbol{c}-\theta\hat{\boldsymbol{x}})^{\text{T}}\bar{\boldsymbol{x}}\,|\,\bar{\boldsymbol{x}}\in L\right\} \tag{28}$$

which is solved by the method presented in Appendix A.

As for the convergence, the procedure is terminated as soon as the infeasibility for the conic constraints is less than a threshold:

$$\sum\max\{0,P_{\text{in}\,i,t}^2+Q_{\text{in}\,i,t}^2-v_{\text{in}\,i,t}u_{i,t}\}\le\delta \tag{29}$$

The most computationally demanding part of the algorithm is the solution to the LP problem (28). The proposed distributed and parallel procedure is based on a modified version of the method proposed in [29] and is explained in Appendix A. This method scales to much higher dimensions when compared with the ADMM-based parallelized version of the method known as the splitting conic solver [33].

Once problem (28) is solved, dual variables λ corresponding to $\boldsymbol{Ax}=\boldsymbol{b}$ are obtained. The prices of transactions between LEC prosumers are obtained by computing the shadow prices derived from (20).

C. Privacy Preservation Strategy

Since conic constraints in (11) are local ones, the optimization for each user can be private without disclosing any data to others. Once the optimization is conducted for all users, the new solution is fed into the penalized LP, and the LP is solved while preserving privacy as described in [28]. Using similar notations as in [28], (28) can be rewritten as:

$$\begin{cases} \min \boldsymbol{c}^{\mathrm{T}}\boldsymbol{x} \\ \text{s.t. } \overline{\boldsymbol{A}}_1\boldsymbol{x}_1+\overline{\boldsymbol{A}}_2\boldsymbol{x}_2+\ldots+\overline{\boldsymbol{A}}_n\boldsymbol{x}_n=\overline{\boldsymbol{b}} \\ \quad \hat{\boldsymbol{A}}_{ii}\boldsymbol{x}_i=\hat{\boldsymbol{b}}_i \quad i=1,2,\ldots,n \\ \quad \boldsymbol{lb}\le\boldsymbol{x}\le\boldsymbol{ub} \end{cases} \tag{30}$$

where $\boldsymbol{x}_1,\boldsymbol{x}_2,\ldots,\boldsymbol{x}_n$ are n vectors of unknown variables.

The global and local constraints are denoted as $\overline{\boldsymbol{A}}_1\boldsymbol{x}_1+\overline{\boldsymbol{A}}_2\boldsymbol{x}_2+\ldots+\overline{\boldsymbol{A}}_n\boldsymbol{x}_n=\overline{\boldsymbol{b}}$ and $\hat{\boldsymbol{A}}_{ii}\boldsymbol{x}_i=\hat{\boldsymbol{b}}_i, i=1,2,\ldots,n$, respectively.

$$\begin{cases} \boldsymbol{A}=\begin{bmatrix} \overline{\boldsymbol{A}}_1 & \overline{\boldsymbol{A}}_2 & \ldots & \overline{\boldsymbol{A}}_n \\ \hat{\boldsymbol{A}}_{11} & \hat{\boldsymbol{A}}_{12} & \ldots & \hat{\boldsymbol{A}}_{1n} \\ \vdots & \vdots & & \vdots \\ \hat{\boldsymbol{A}}_{n1} & \hat{\boldsymbol{A}}_{n2} & \ldots & \hat{\boldsymbol{A}}_{nn} \end{bmatrix} \\ \boldsymbol{b}=\begin{bmatrix} \overline{\boldsymbol{b}} \\ \hat{\boldsymbol{b}}_1 \\ \vdots \\ \hat{\boldsymbol{b}}_n \end{bmatrix} \end{cases} \tag{31}$$

in which $\hat{\boldsymbol{A}}_{ij}=\boldsymbol{0}$ for $i\neq j$:

$$\begin{bmatrix} \overline{\boldsymbol{A}}_1 & \overline{\boldsymbol{A}}_2 & \ldots & \overline{\boldsymbol{A}}_n \\ \hat{\boldsymbol{A}}_{11} & \hat{\boldsymbol{A}}_{12} & \ldots & \hat{\boldsymbol{A}}_{1n} \\ \vdots & \vdots & & \vdots \\ \hat{\boldsymbol{A}}_{n1} & \hat{\boldsymbol{A}}_{n2} & \ldots & \hat{\boldsymbol{A}}_{nn} \end{bmatrix}^{\mathrm{T}}\begin{bmatrix} \xi_0 \\ \xi_1 \\ \vdots \\ \xi_n \end{bmatrix}=\begin{bmatrix} \overline{\boldsymbol{A}}_1^{\mathrm{T}}\xi_0+\hat{\boldsymbol{A}}_{11}^{\mathrm{T}}\xi_1 \\ \overline{\boldsymbol{A}}_2^{\mathrm{T}}\xi_0+\hat{\boldsymbol{A}}_{22}^{\mathrm{T}}\xi_2 \\ \vdots \\ \overline{\boldsymbol{A}}_n^{\mathrm{T}}\xi_0+\hat{\boldsymbol{A}}_{nn}^{\mathrm{T}}\xi_n \end{bmatrix} \tag{32}$$

Step 3 of the procedure presented in [28] can be rewritten as:

$$\boldsymbol{x}(\xi)=-\frac{\boldsymbol{A}^{\mathrm{T}}\boldsymbol{\xi}+\boldsymbol{c}-\theta\hat{\boldsymbol{x}}}{\gamma}=\begin{bmatrix} -\dfrac{\overline{\boldsymbol{A}}_1^{\mathrm{T}}\xi_0}{\gamma}-\dfrac{\hat{\boldsymbol{A}}_{11}^{\mathrm{T}}\xi_1}{\gamma}+\dfrac{\theta\hat{\boldsymbol{x}}_1-\boldsymbol{c}_1}{\gamma} \\ -\dfrac{\overline{\boldsymbol{A}}_2^{\mathrm{T}}\xi_0}{\gamma}-\dfrac{\hat{\boldsymbol{A}}_{22}^{\mathrm{T}}\xi_2}{\gamma}+\dfrac{\theta\hat{\boldsymbol{x}}_2-\boldsymbol{c}_2}{\gamma} \\ \vdots \\ -\dfrac{\overline{\boldsymbol{A}}_n^{\mathrm{T}}\xi_0}{\gamma}-\dfrac{\hat{\boldsymbol{A}}_{nn}^{\mathrm{T}}\xi_n}{\gamma}+\dfrac{\theta\hat{\boldsymbol{x}}_n-\boldsymbol{c}_n}{\gamma} \end{bmatrix} \tag{33}$$

The i^{th} user can update its configuration $\boldsymbol{x}_i(\boldsymbol{\xi})$ without exchanging the information about its objective function $\boldsymbol{c}_i$, the dual variables $\boldsymbol{\xi}_i$, or the projected primal $\hat{\boldsymbol{x}}_i$.

IV. Test Results

The proposed method has been implemented in MATLAB R2022b on a computer with an Intel(R) Core(TM) i7-10700 CPU @ 2.90 GHz with 16 GB of RAM and running 64-bit Windows 11.

Two test systems have been considered to validate the proposed method.

1) A 14-bus distribution network with 23 kV rated voltage and three feeders (data are given in [34]).

2) An 84-bus distribution network with 11.4 kV rated voltage and 11 feeders (data are given in [35]).

Twenty-four periods of 1 hour each are considered during the single-day horizon for both test systems.

To verify the effectiveness of the proposed method, three cases have been compared.

1) Case 1: energy exchanges do not occur among prosumers.

2) Case 2: prosumers are allowed to exchange energy within the LEC (connected feeders).

3) Case 3: direct exchanges are allowed only among prosumers belonging to the same feeder by implementing constraint (7) independently for each feeder (separate feeders).

Table II lists the battery sizes considered in the two test systems. The battery capacity to rated power ratio is assumed to be 1 hour.

TABLE II
Battery Sizes

Test system	Bus	Size (MWh)	Test system	Bus	Size (MWh)
14-bus distribution network	1	0.5	84-bus distribution network	2	0.48
	2	0.3		9	0.48
	3	0.4		14	0.48
	4	0.2		27	0.56
	5	0.3		32	0.24
	6	1.0		34	0.24
	7	0.5		36	0.24
	8	1.0		38	0.40
	9	0.2		52	0.48
	10	0.6		64	0.40
	11	0.1		66	0.40
	12	0.2		71	0.40
	13	0.2			

For both the 14-bus and 84-bus distribution networks, the solutions obtained by using the proposed method combining CP and LP are compared with those provided by the centralized optimization proposed in [31] and [32] and implemented in MATLAB. The results derived from the proposed method are labeled "D", whereas those obtained by the centralized optimization are labeled "C" in Tables III and IV.

TABLE III
COMPARISON OF PROPOSED METHOD WITH CENTRALIZED OPTIMIZATION FOR 14-BUS DISTRIBUTION NETWORK

Case	*OF* (k€)		Augmented *OF* (k€)		Loss (MWh)	
	C	D	C	D	C	D
Case 1	41.7	41.7	41.7	41.7	3.38	3.38
Case 2	37.1	37.1	37.1	37.1	4.40	4.40
Case 3	39.2	39.2	39.2	39.2	4.77	4.77

TABLE IV
COMPARISON OF PROPOSED METHOD WITH CENTRALIZED OPTIMIZATION FOR 84-BUS DISTRIBUTION NETWORK

Case	*OF* (k€)		Augmented *OF* (k€)		Loss (MWh)	
	C	D	C	D	C	D
Case 1	36.5	36.5	36.5	36.5	4.5	4.5
Case 2	28.8	28.8	28.8	28.8	4.8	4.8
Case 3	30.0	30.0	30.0	30.0	4.9	4.9

A. Test Results on 14-bus Distribution Network

The 14-bus distribution network consists of three feeders. At each bus, a prosumer is endowed with a PV system and battery system. Prosumers with different profiles for load and PV production are assumed. The total daily energy consumptions of the LEC and PV production are equal to 195 MWh and 84 MWh (43% of the load), respectively. Load and PV production profiles are shown in Fig. 2(a) and (b), respectively, where the colored lines refer to different prosumers located at different buses. The total capacity of the batteries is 8.25 MWh (9.8% of the daily PV production).

Figure 3 shows the profiles of the prices of the energy bought/sold from/to the main grid, i.e., π_{buy} and π_{sell}, respectively, together with the energy prices of the exchanges between prosumers while considering connected feeders, i. e., case 2. Colors solely depict the 3-D nature of the surface, which applies to all the subsequent figures. Very similar results are obtained in terms of the objective function, power losses, voltage profiles, prosumer power exchanges, and currents for cases 1-3. The objective function, which is equal to €41.7×10^3 in case 1, decreases to €37.1×10^3 in case 2 and to €39.2×10^3 in case 3. A comparison of the objective function with the augmented one shows that the additional penalization terms included in the objective function (25) are close to zero for all cases. As Table III shows, the proposed method can achieve the same optimal values for the objective function when compared with the centralized optimization proposed in [31], [32].

Because of the energy exchanges among prosumers, the energy costs reduce to approximately €4600 (11%) and approximately €2500 (6%) in the cases of connected and separated feeders, respectively, when compared with the case without P2P energy exchanges.

Voltage profiles and currents in the 14-bus distribution network are shown for case 1 in Figs. 4 and 5, respectively.

Energy exchanges determine an increase in power losses of approximately 30% and 41% in the cases of connected and separated feeders, respectively, when compared with the case without energy exchanges (case 1).

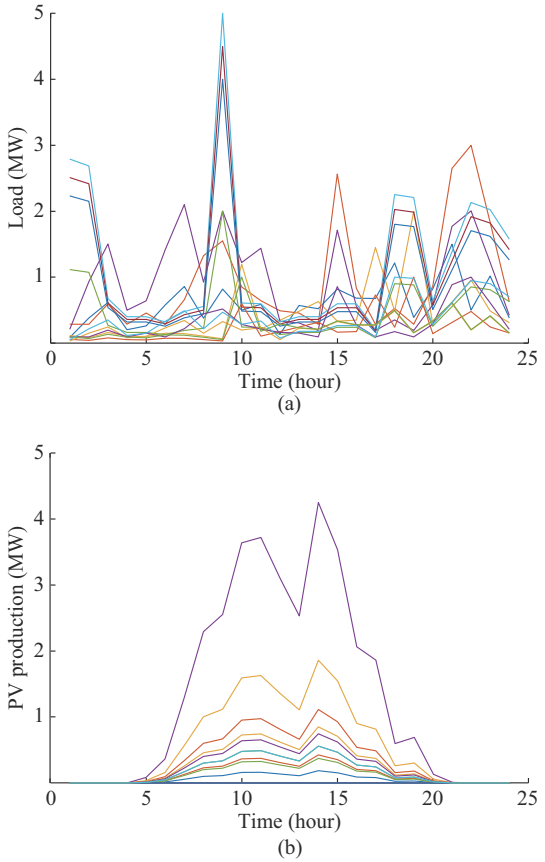

Fig. 2. Prosumer characteristics for 14-bus distribution network. (a) Load profiles. (b) PV production profiles for each prosumer.

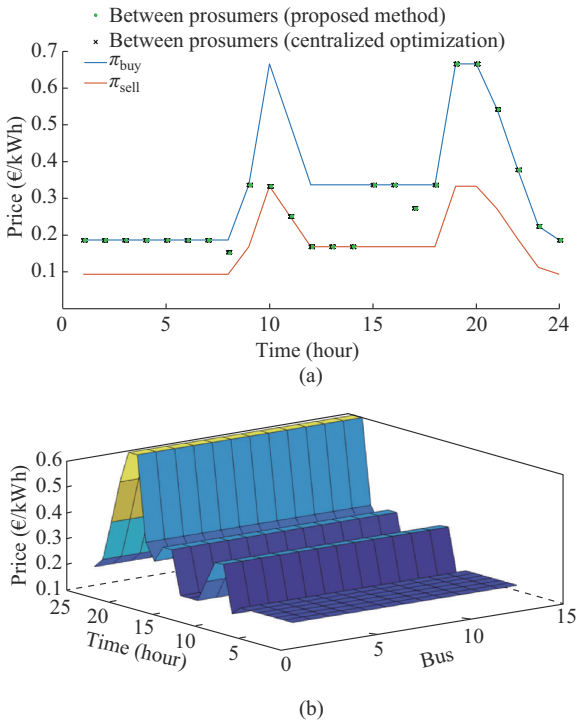

Fig. 3. Energy prices with connected feeders (case 2). (a) Profiles of prices of transaction with utility grid and energy prices of exchanges between prosumers. (b) Energy prices of exchanges between prosumers at different buses.

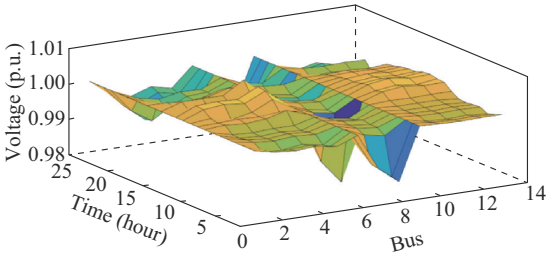

Fig. 4. Voltages in 14-bus distribution network.

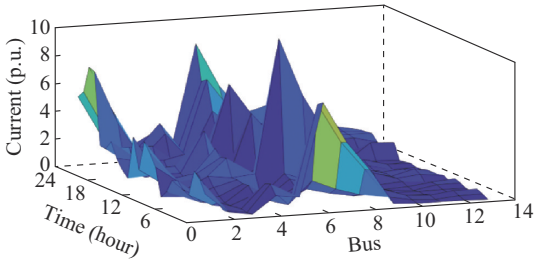

Fig. 5. Currents in 14-bus distribution network.

P2P energy exchanges are, indeed, higher in the case with connected feeders as compared with those with separated feeders (case 3), as shown in Fig. 6.

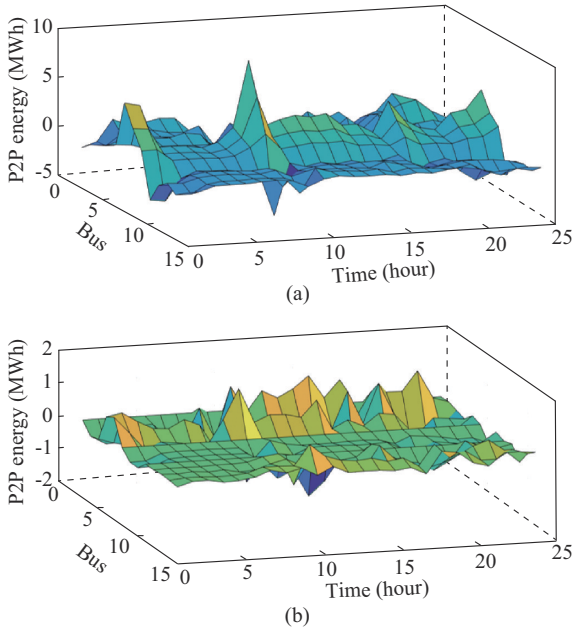

Fig. 6. P2P energy exchange among prosumers for 14-bus distribution network. (a) With connected feeders (case 2). (b) With separated feeders (case 3).

Figure 7 shows that energy exchanges with the main grid diminish due to P2P energy exchanges among prosumers. Prosumers endowed with batteries can reduce the amount of energy exchanged with the main grid to a much greater extent due to the optimal management of the batteries, as shown in Fig. 8, which allows better exploitation of the energy produced by PV systems and an increase in the energy self-consumption in the LEC.

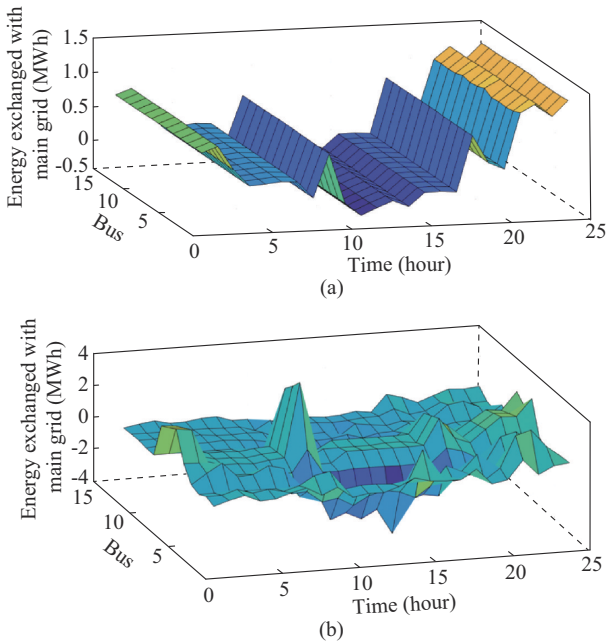

Fig. 7. Energy exchanged with main grid for 14-bus distribution network. (a) With P2P energy exchanges among prosumers (case 2). (b) Without energy exchanges among prosumers (case 1).

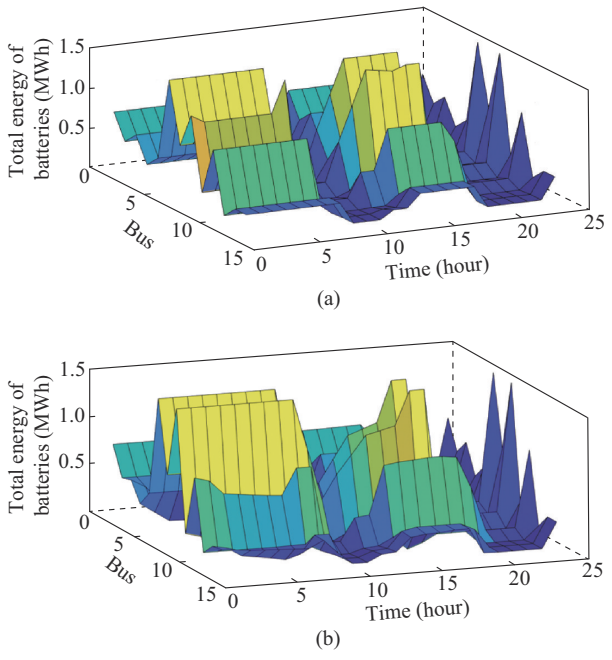

Fig. 8. Total energy of batteries for 14-bus distribution network. (a) With energy exchanges among prosumers (case 2). (b) Without energy exchanges among prosumers (case 1).

B. Test Results on 84-bus Distribution Network

The 84-bus distribution network is illustrated in Fig. 9. Several prosumers are endowed with a PV system and a battery.

Load and PV production profiles are shown in Fig. 10(a) and (b), respectively. The total daily energy consumptions of the LEC and PV production are equal to 239 MWh and 178 MWh (74.4% of the load), respectively. The total capacity of the batteries is 4.8 MWh (3.2% of the daily PV production).

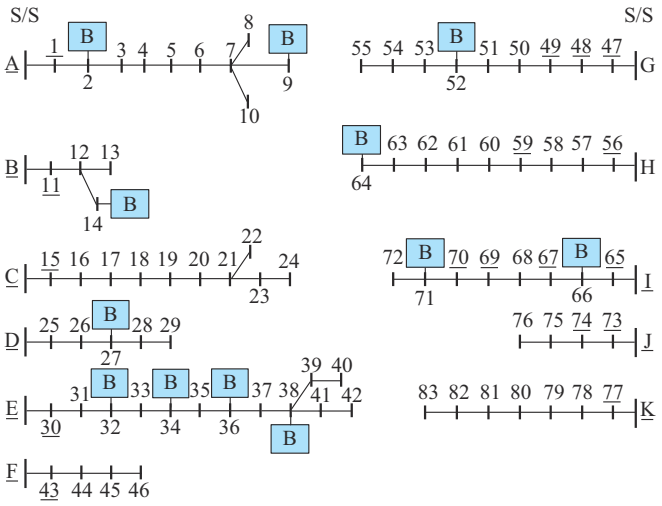

Fig. 9. 84-bus distribution network.

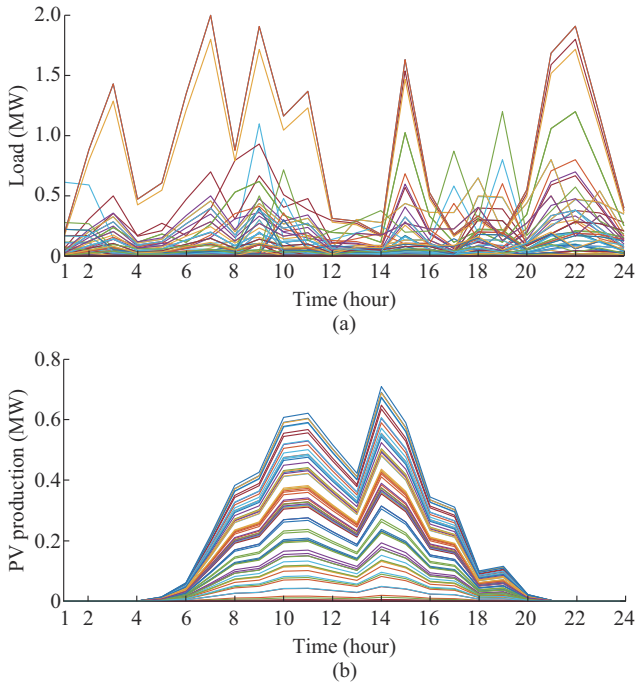

Fig. 10. Prosumer characteristics for 84-bus distribution network. (a) Load profiles. (b) PV production profiles for each prosumer.

Figures 11 and 12 show the assumed profiles of the price of the energy bought/sold from/to the main grid (i.e., π_{buy} and π_{sell}, respectively) together with the energy prices of the exchanges between prosumers (indicated as prices between prosumers) when considering connected and separated feeders, i.e., cases 2 and 3, respectively. It is worth noting that the prices of the internal P2P transactions and the corresponding dual variables associated with the power equilibrium constraints of the proposed method are essentially the same as those of the centralized optimization in both cases.

In the case of connected feeders, as shown in Fig. 11, the energy prices of the exchanges between prosumers mainly coincide with the prices of the energy bought/sold from/to the main grid for all buses. When the LEC globally imports/exports electricity from/to the utility grid, the prices of the internal transactions align with $\pi_{\text{buy},t}$ or $\pi_{\text{sell},t}$.

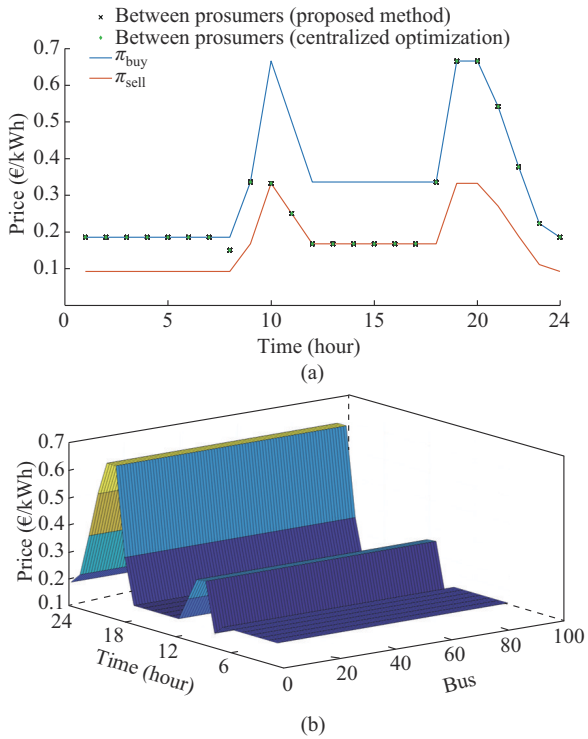

Fig. 11. Energy prices with connected feeders (case 2) for 81-bus distribution network. (a) Profiles of prices of transactions with utility grid and energy prices of exchanges between prosumers. (b) Energy prices of exchanges between prosumers at different buses.

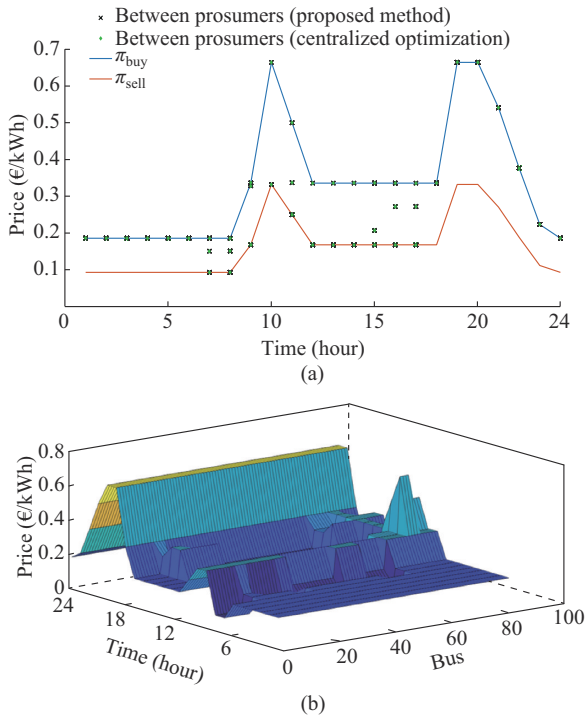

Fig. 12. Energy prices with separated feeders (case 3) for 81-bus distribution network. (a) Profiles of prices of transactions with utility grid and energy prices of exchanges between prosumers. (b) Energy prices of exchanges between prosumers at different buses.

In the case of separated feeders, as shown in Fig. 12, the energy prices of the exchanges between prosumers show a more variable behavior. The sizes and locations of PV/battery systems influence the prices related to the energy exchanges so that the prosumers connected at buses closer to PV/battery systems tend to exchange the energy at lower prices. This is more evident for the prosumers located at feeder K for which the installed capacity of PV systems is lower than that of other feeders and the battery systems are not installed.

When comparing the values of the objective function in the three cases, the best value is achieved in case 2, as shown in Table IV. In addition, a comparison of the objective function with the augmented one shows that the additional penalization terms included in the objective function (25) are close to zero for all cases. As shown in Table IV, the proposed method can achieve the same optimal values for the objective function when compared with the centralized optimization proposed in [31], [32].

The CPU time required by the sequential computing procedure is less than 8 s.

As expected, the energy exchanges among prosumers enable a significant reduction in energy costs, that is, approximately €7700 (21%) and approximately €6500 (18%) in the case of connected and separated feeders, respectively, when compared with the case without P2P energy exchanges.

As regard power losses in the branches of the internal network, energy exchanges lead to increases of approximately 7% (approximately 300 kWh) and 9% in the case of connected (case 2) and separated feeders, respectively, when compared with the case without energy exchanges (case 1). Energy exchanges are indeed higher in the case with connected feeders than with separated feeders (case 3), as shown in Fig. 13.

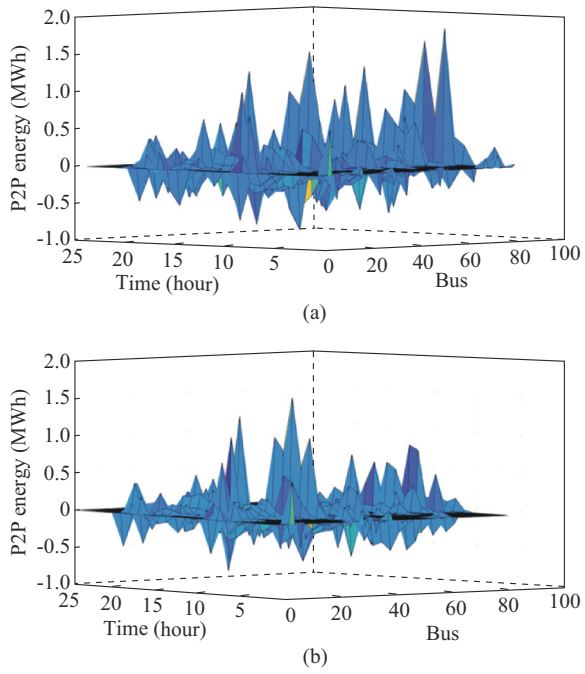

Fig. 13. P2P energy exchanges among prosumers for 81-bus distribution network. (a) With connected feeders (case 2). (b) With separated feeders (case 3).

Figure 14 shows the reduction in energy exchanged with the main grid due to the energy transactions among prosumers. The benefits derived from the energy exchanges are more evident for prosumers endowed with batteries because of the flexibility offered by optimal storage operation. The total energy of batteries is shown in Fig. 15(a) and (b) for cases 2 and 1, respectively. The optimal operation of batteries supports the energy exchanges among prosumers during the day and contributes to more efficient usage of the energy produced by PV systems, thus increasing the energy self-consumption in the LEC.

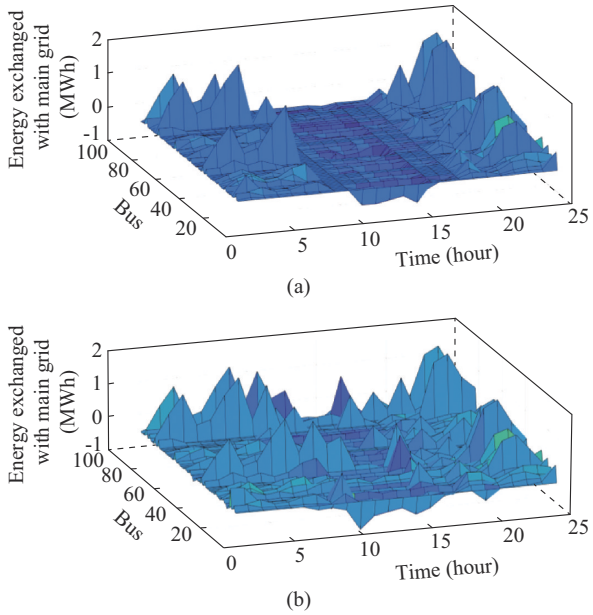

Fig. 14. Reduction in energy exchanged with main grid. (a) With P2P energy exchanges among prosumers (case 2). (b) Without energy exchanges among prosumers (case 1).

V. Conclusion

This paper presents a novel iterative two-stage optimization method that combines LP and a new CP procedure for scheduling LECs while considering network constraints and branch power losses. CP procedures are conducted locally for each prosumer, enabling the computational burden to be equally distributed. The method is highly scalable and has features that can be implemented on microcontrollers, as both LP and CP procedures require only simple matrix-vector multiplication.

Simulation results demonstrate that the proposed method is computationally efficient, achieving the same quality of solutions as that by centralized optimization in a few seconds. The prices of energy transactions among prosumers are also calculated. Participation in a LEC is convenient for each prosumer, with individual economic benefits mainly derived from the sizes and locations of the PV/battery systems in the network.

Future works will focus on the benefits of providing ancillary services to system operators and on real-time optimization of the LECs [36] while considering prosumer rights related to carbon emissions [37]. Prosumers can improve their economic benefits by also providing up- or down-regulation [27].

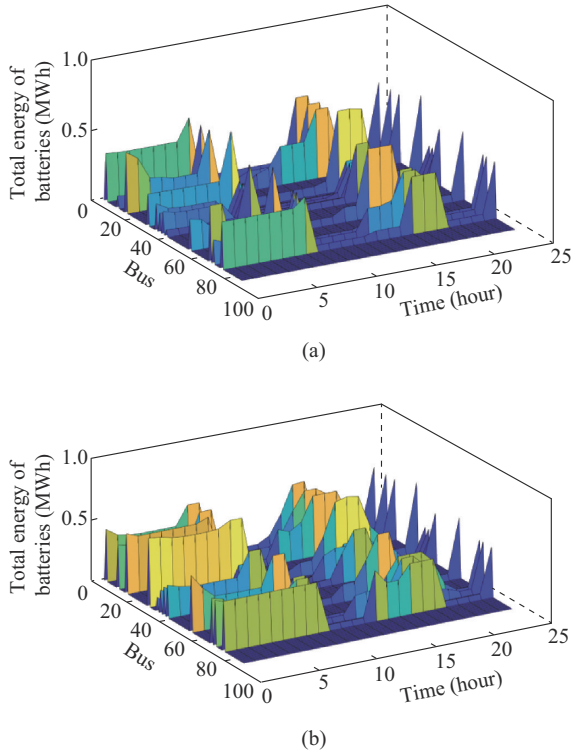

Fig. 15. Total energy of batteries for 84-bus distribution network. (a) With energy exchanges among prosumers (case 2). (b) Without energy exchanges among prosumers (case 1).

APPENDIX A

A. Matrix Free LP Solver

The advantage of the accelerated gradient descent (AGD) method for solving LPs is that it relies merely on matrix-vector multiplications, which are parallelizable and can be carried out in a privacy-preserving way.

Considering the generic LP problem $\min \boldsymbol{c}^{\mathrm{T}}\boldsymbol{x}\boldsymbol{A}\boldsymbol{x}=\boldsymbol{b}, \boldsymbol{lb}\le\boldsymbol{x}\le\boldsymbol{ub}$, the lagrangian dual is:

$$\max_{\boldsymbol{\lambda}} \min_{\boldsymbol{lb}\le\boldsymbol{x}\le\boldsymbol{ub}} \{\boldsymbol{c}^{\mathrm{T}}\boldsymbol{x}+\boldsymbol{\lambda}^{\mathrm{T}}(\boldsymbol{A}\boldsymbol{x}-\boldsymbol{b})\} \tag{A1}$$

Following [29], to guarantee that, for a given value of $\boldsymbol{\lambda}$, the unconstrained version of the inner optimization has a unique solution $\boldsymbol{x}(\boldsymbol{\lambda})$, a quadratic penalization term is added to the Lagrangian dual problem:

$$\max_{\boldsymbol{\lambda}} \min_{\boldsymbol{lb}\le\boldsymbol{x}\le\boldsymbol{ub}} \left\{\boldsymbol{c}^{\mathrm{T}}\boldsymbol{x}+\frac{\gamma}{2}\boldsymbol{x}^{\mathrm{T}}\boldsymbol{x}+\boldsymbol{\lambda}^{\mathrm{T}}(\boldsymbol{A}\boldsymbol{x}-\boldsymbol{b})\right\} \tag{A2}$$

where $\gamma>0$ is a parameter. When γ is very small, (A2) gets very close to (A1) and gives a good approximate solution.

By denoting $f(\boldsymbol{\lambda})=\min_{\boldsymbol{lb}\le\boldsymbol{x}\le\boldsymbol{ub}}\left\{\boldsymbol{c}^{\mathrm{T}}\boldsymbol{x}+\frac{\gamma}{2}\boldsymbol{x}^{\mathrm{T}}\boldsymbol{x}+\boldsymbol{\lambda}^{\mathrm{T}}(\boldsymbol{A}\boldsymbol{x}-\boldsymbol{b})\right\}$, (A2) can be written as:

$$\max_{\boldsymbol{\lambda}} f(\boldsymbol{\lambda}) \tag{A3}$$

Problem (A3) can be solved by any first-order methods (FOMs) such as the gradient descent (GD), the main steps of which are presented in GD algorithm, where η is the step size.

Algorithm A1: gradient descent algorithm

Step 1: start with an initial guess $\boldsymbol{\lambda}$
Step 2: while $\|\nabla f(\boldsymbol{\lambda})\|$ is bigger than a threshold do:
Step 3: $\boldsymbol{\lambda}=\boldsymbol{\lambda}+\eta\nabla f(\boldsymbol{\lambda})$
Step 4: end

Because the minimum of $\boldsymbol{c}^{\mathrm{T}}\boldsymbol{x}+\frac{\gamma}{2}\boldsymbol{x}^{\mathrm{T}}\boldsymbol{x}+\boldsymbol{\lambda}^{\mathrm{T}}(\boldsymbol{A}\boldsymbol{x}-\boldsymbol{b})$ for a fixed $\boldsymbol{\lambda}$ is reached when $\frac{\partial}{\partial\boldsymbol{x}}\left(\boldsymbol{c}^{\mathrm{T}}\boldsymbol{x}+\frac{\gamma}{2}\boldsymbol{x}^{\mathrm{T}}\boldsymbol{x}+\boldsymbol{\lambda}^{\mathrm{T}}(\boldsymbol{A}\boldsymbol{x}-\boldsymbol{b})\right)=\boldsymbol{0}$ or $\boldsymbol{c}+\gamma\boldsymbol{x}+\boldsymbol{A}^{\mathrm{T}}\boldsymbol{\lambda}=\boldsymbol{0}$,

$$\boldsymbol{x}(\boldsymbol{\lambda})=-\frac{\boldsymbol{A}^{\mathrm{T}}\boldsymbol{\lambda}+\boldsymbol{c}}{\gamma} \tag{A4}$$

In contrast with ADMM-based methods, expensive intermediate steps are avoided.

Following [38], a good estimate for $f(\boldsymbol{\lambda})$ can be obtained by the projection of $\boldsymbol{x}(\boldsymbol{\lambda})$ onto $\{\boldsymbol{x}\,|\,\boldsymbol{lb}\le\boldsymbol{x}\le\boldsymbol{ub}\}$, by setting $\boldsymbol{x}_i(\boldsymbol{\lambda})=\boldsymbol{ub}(i)$ if $\boldsymbol{x}_i(\boldsymbol{\lambda})>\boldsymbol{ub}(i)$, $\boldsymbol{x}_i(\boldsymbol{\lambda})=\boldsymbol{lb}(i)$ if $\boldsymbol{x}_i(\boldsymbol{\lambda})<\boldsymbol{lb}(i)$, and by leaving the values $\boldsymbol{x}_i(\boldsymbol{\lambda})$ within the boundaries unchanged:

$$\boldsymbol{x}_i(\boldsymbol{\lambda})=\min(\boldsymbol{x}_i(\boldsymbol{\lambda}),\boldsymbol{ub}(i)) \tag{A5}$$

$$\boldsymbol{x}_i(\boldsymbol{\lambda})=\max(\boldsymbol{x}_i(\boldsymbol{\lambda}),\boldsymbol{lb}(i)) \tag{A6}$$

Moreover, since $\frac{\partial}{\partial\boldsymbol{\lambda}}\left(\boldsymbol{c}^{\mathrm{T}}\boldsymbol{x}+\frac{\gamma}{2}\boldsymbol{x}^{\mathrm{T}}\boldsymbol{x}+\boldsymbol{\lambda}^{\mathrm{T}}(\boldsymbol{A}\boldsymbol{x}-\boldsymbol{b})\right)=\boldsymbol{A}\boldsymbol{x}-\boldsymbol{b}$,

$$\nabla f(\boldsymbol{\lambda})=\boldsymbol{A}\boldsymbol{x}(\boldsymbol{\lambda})-\boldsymbol{b} \tag{A7}$$

As explained in [29], a fixed step size $\eta=L=\frac{\gamma}{\|\boldsymbol{A}\|_S^2}$ can be adopted, in which $\|\boldsymbol{A}\|_S^2$ is the maximum eigenvalue of $\boldsymbol{A}^{\mathrm{T}}\boldsymbol{A}$ [39]. By applying AGD [29], [40], a two-step updating rule of the dual vector $\boldsymbol{\lambda}^{k+1}$ is implemented:

$$\begin{cases}\boldsymbol{\lambda}^{k+1}:=\max(0,\boldsymbol{\xi}^k+\eta\nabla(\boldsymbol{\xi}^k))\\ \boldsymbol{\xi}^{k+1}:=\boldsymbol{\lambda}^k+\beta_k(\boldsymbol{\lambda}^k-\boldsymbol{\lambda}^{k-1})\end{cases} \tag{A8}$$

where $\beta_k=\frac{2(t_k-1)}{1+\sqrt{1+4t_k^2}}$ with initial parameters $t_1=1$ and $\xi^1=\lambda^0$.

AGD guarantees a $O(1/k^2)$ convergence rate which means: $f^*-f(\boldsymbol{\lambda}^k)\le O(1/k^2)$.

The details of accelerated gradient descent algorithm for LP are presented in the following algorithm.

B. Exact Conic Projection

If $\mathbb{C}$ is a convex set, the projection of $\boldsymbol{x}$ onto $\mathbb{C}$ is $\hat{\boldsymbol{x}}=\arg\min_{\boldsymbol{x}\in\mathbb{C}}\|\boldsymbol{x}-x_0\|$, which is the closest point $\boldsymbol{x}$ in $\mathbb{C}$ to x_0.

We consider the case in which $\mathbb{C}$ is the second-order cone [41] $\mathbb{C}=\{(\boldsymbol{w},t)|(\boldsymbol{w},t)\in\mathbb{R}^n\times\mathbb{R}^+,\|\boldsymbol{w}\|\le t\}$. $\mathbb{C}$ is convex. Indeed, having $(w_1,t_1)\in\mathbb{C}$ and $(w_2,t_2)\in\mathbb{C}$ implies that $\|w_1\|\le t_1$ and $\|w_2\|\le t_2$, respectively [38]. If each of the later inequalities is multiplied by θ and $1-\theta$, respectively (in which $\theta\in[0,1]$) and then, they are summed up, $\|\theta w_1\|+\|(1-\theta)w_2\|\le\theta t_1+(1-\theta)t_2$ is obtained. From triangle inequality, $\|\theta w_1+(1-\theta)w_2\|\le\|\theta w_1\|+\|(1-\theta)w_2\|$ and then $\|\theta w_1+(1-\theta)w_2\|\le\theta t_1+(1-\theta)t_2$ which in turn indicates that $(\theta w_1+(1-\theta)w_2,\theta t_1+(1-\theta)t_2)=\theta(w_1,t_1)+(1-\theta)(w_2,t_2)\in\mathbb{C}$, which corresponds to the definition of convex sets.

Algorithm A2: accelerated gradient descent algorithm for LP

Step 1: start with an initial guess $\boldsymbol{\lambda}$
Step 2: $L=\frac{\gamma}{\|\boldsymbol{A}\|_S^2}, \boldsymbol{\zeta}=\boldsymbol{\lambda}, t_k=1$
Step 3: $\boldsymbol{x}(\boldsymbol{\zeta})=-\frac{\boldsymbol{A}^{\mathrm{T}}\boldsymbol{\zeta}+\boldsymbol{c}}{\gamma}$
Step 4: $\boldsymbol{x}(\boldsymbol{\zeta})=\max(\boldsymbol{lb},\boldsymbol{x}(\boldsymbol{\zeta}))$
Step 5: $\boldsymbol{x}(\boldsymbol{\zeta})=\min(\boldsymbol{ub},\boldsymbol{x}(\boldsymbol{\zeta}))$
Step 6: $\nabla f(\boldsymbol{\zeta})=\boldsymbol{A}\boldsymbol{x}(\boldsymbol{\zeta})-\boldsymbol{b}$
Step 7: while $\|\nabla f(\boldsymbol{\zeta})\|$ is bigger than a threshold do:
Step 8: $\boldsymbol{\lambda}_{old}=\boldsymbol{\lambda}$
Step 9: $\boldsymbol{x}(\boldsymbol{\zeta})=-\frac{\boldsymbol{A}^{\mathrm{T}}\boldsymbol{\zeta}+\boldsymbol{c}}{\gamma}$
Step 10: $\boldsymbol{x}(\boldsymbol{\zeta})=\max(\boldsymbol{lb},\boldsymbol{x}(\boldsymbol{\zeta}))$
Step 11: $\boldsymbol{x}(\boldsymbol{\zeta})=\min(\boldsymbol{ub},\boldsymbol{x}(\boldsymbol{\zeta}))$
Step 12: $\nabla f(\boldsymbol{\zeta})=\boldsymbol{A}\boldsymbol{x}(\boldsymbol{\zeta})-\boldsymbol{b}$
Step 13: $\boldsymbol{\lambda}=\max(0,\boldsymbol{\zeta}+L\nabla f(\boldsymbol{\zeta}))$
Step 14: $\beta=\frac{2(t_k-1)}{1+\sqrt{1+4t_k^2}}$
Step 15: $t_k=\frac{1+\sqrt{1+4t_k^2}}{2}$
Step 16: $\boldsymbol{\xi}=\boldsymbol{\lambda}+\beta(\boldsymbol{\lambda}-\boldsymbol{\lambda}_{old})$
Step 17: end

The constraint of the form $\boldsymbol{u}^{\mathrm{T}}\boldsymbol{u}\le xy$ in which $x,y\in\mathbb{R}^+$ and $\boldsymbol{u}\in\mathbb{R}^n$ can be written as $4\boldsymbol{u}^{\mathrm{T}}\boldsymbol{u}-2xy\le 2xy$ and then $4\boldsymbol{u}^{\mathrm{T}}\boldsymbol{u}+x^2-2xy+y^2\le x^2+2xy+y^2$ or $4\boldsymbol{u}^{\mathrm{T}}\boldsymbol{u}+(x-y)^2\le(x+y)^2$, which, after taking the square root of both hand sides, can be written in matrix form as $\left\|\begin{matrix}2\boldsymbol{u}\\ x-y\end{matrix}\right\|\le x+y$, i. e., a second-order cone. If $(z,w)\in\mathbb{R}^+\times\mathbb{R}^+$ and $\boldsymbol{u}=\begin{bmatrix}z\\ w\end{bmatrix}$, $\boldsymbol{u}^{\mathrm{T}}\boldsymbol{u}=z^2+w^2$. Therefore, $\mathbb{C}=\{(x,y,z,w)|(x,y,z,w)\in\mathbb{R}^+\times\mathbb{R}^+\times\mathbb{R}\times\mathbb{R},\ z^2+w^2\le xy\}$, called the rotated second-order cone, is a convex set [41].

Project of a given point $(x_0,y_0,z_0,w_0)\notin\mathbb{C}$ onto $\mathbb{C}$, the closest point (x,y,z,w) in $\mathbb{C}$ to (x_0,y_0,z_0,w_0) lies on the boundary of $\mathbb{C}$ which means $xy=z^2+w^2$. So the following optimization problem needs to be solved:

$$\begin{cases}\min[(x-x_0)^2+(y-y_0)^2+(z-z_0)^2+(w-w_0)^2]\\ \text{s.t. } xy=z^2+w^2\end{cases}\tag{B1}$$

The above optimization is solved by using the Lagrangian method of multipliers. The lagrangian is:

$$\begin{aligned}L(x,y,z,w,\lambda)=&(x-x_0)^2+(y-y_0)^2+(z-z_0)^2+\\&(w-w_0)^2+\lambda(z^2+w^2-xy)\end{aligned}\tag{B2}$$

for which equilibrium points satisfy the following conditions:

$$\frac{\partial L}{\partial x}=2(x-x_0)-\lambda y=0\tag{B3}$$

$$\frac{\partial L}{\partial y}=2(y-y_0)-\lambda x=0\tag{B4}$$

$$\frac{\partial L}{\partial z}=2(z-z_0)+2\lambda z=0\tag{B5}$$

$$\frac{\partial L}{\partial w}=2(w-w_0)+2\lambda w=0\tag{B6}$$

$$\frac{\partial L}{\partial \lambda}=z^2+w^2-xy=0\tag{B7}$$

From (B5) and (B6), respectively, we can obtain:

$$z(\lambda)=\frac{z_0}{1+\lambda}\tag{B8}$$

$$w(\lambda)=\frac{w_0}{1+\lambda}\tag{B9}$$

From (44), we can obtain:

$$y=\frac{2(x-x_0)}{\lambda}\tag{B10}$$

From (51) and (45), we can obtain:

$$x(\lambda)=2\frac{2x_0+\lambda y_0}{4-\lambda^2}\tag{B11}$$

and, similarly,

$$y(\lambda)=2\frac{2y_0+\lambda x_0}{4-\lambda^2}\tag{B12}$$

The solution of the system of nonlinear equations (B3) - (B7) provides λ, which is used in (B8), (B9), (B11), and (B12) to compute x, y, z and w, i. e., the optimal solution to (B1).

The value of λ is obtained by the roots of a 4th-order polynomial. Indeed, from (B7) - (B9), (B11), and (B12), as $xy=z^2+w^2$, we can obtain:

$$4\frac{(2x_0+\lambda y_0)(2y_0+\lambda x_0)}{(4-\lambda^2)^2}=\frac{z_0^2+w_0^2}{(1+\lambda)^2}\tag{B13}$$

This yields:

$$\begin{aligned}&(4x_0y_0-z_0^2-w_0^2)\lambda^4+8(x_0^2+y_0^2+x_0y_0)\lambda^3+\\&\quad(20x_0y_0+16(x_0^2+y_0^2)+8(z_0^2+w_0^2))\lambda^2+[8(x_0^2+y_0^2)+\\&\quad 32x_0y_0]\lambda+16(x_0y_0-z_0^2-w_0^2)=0\end{aligned}\tag{B14}$$

REFERENCES

[1] B. P. Koirala, E. Koliou, J. Friege *et al*., "Energetic communities for community energy: a review of key issues and trends shaping integrated community energy systems," *Renewable and Sustainable Energy Reviews*, vol. 56, pp. 722-744, Apr. 2016.

[2] P. Siano and D. Mohammad, "MILP Optimization model for assessing the participation of distributed residential PV-battery systems in ancillary services market," *CSEE Journal of Power and Energy Systems*, vol. 7, no. 2, pp. 348-357, Aug. 2020.

[3] A. Paudel, K. Chaudhari, C. Long *et al*., "Peer-to-peer energy trading in a prosumer-based community microgrid: a game-theoretic model," *IEEE Transactions on Industrial Electronics*, vol. 66, no. 8, pp. 6087-6097, Aug. 2019.

[4] M. Khorasany, Y. Mishra, and G. Ledwich, "A decentralised bilateral energy trading system for peer-to-peer electricity markets," *IEEE Transactions on Industrial Electronics*, vol. 67, no. 6, pp. 4646-4657, Jul. 2019.

[5] M. Khorasany, A. Paudel, R. Razzaghi *et al*., "A new method for peer matching and negotiation of prosumers in peer-to-peer energy markets," *IEEE Transactions on Smart Grid*, vol. 12, no. 3, pp. 2472-2483, Dec. 2020.

[6] K. Zhang, S. Troitzsch, S. Hanif *et al*., "Coordinated market design for peer-to-peer energy trade and ancillary services in distribution grids," *IEEE Transactions on Smart Grid*, vol. 11, no. 4, pp. 2929-2941, Jan. 2020.

[7] J. Guerrero, A. C. Chapman, and G. Verbič, "Decentralized P2P energy trading under network constraints in a low-voltage network," *IEEE Transactions on Smart Grid*, vol. 10, no. 5, pp. 5163-5173, Oct. 2018.

[8] W. Tushar, T. K. Saha, C. Yuen *et al*., "Grid influenced peer-to-peer energy trading," *IEEE Transactions on Smart Grid*, vol. 11, no. 2, pp. 1407-1418, Aug. 2019.

[9] K. Anoh, S. Maharjan, A. Ikpehai *et al*., "Energy peer-to-peer trading in virtual microgrids in smart grids: a game-theoretic approach," *IEEE Transactions on Smart Grid*, vol. 11, no. 2, pp. 1264-1275, Aug. 2019.

[10] C. Mu, T. Ding, Y. Sun *et al*., "Energy block-based peer-to-peer contract trading with secure multi-party computation in nanogrid," *IEEE*

Transactions on Smart Grid, vol. 13, no. 6, pp. 4759-4772, Nov. 2022.
[11] A. Paudel, L. P. M. I. Sampath, J. Yang *et al*., "Peer-to-peer energy trading in smart grid considering power losses and network fees," *IEEE Transactions on Smart Grid*, vol. 11, no. 6, pp. 4727-4737, May 2020.
[12] Y. Sun, X. Wu, J. Wang *et al*., "Power compensation of network losses in a microgrid with BESs by distributed consensus algorithm," *IEEE Transactions on Systems, Man, and Cybernetics: Systems*, vol. 51, no. 4, pp. 2091-2100, Feb. 2020.
[13] J. Kim and Y. Dvorkin, "A P2P-dominant distribution system architecture," *IEEE Transactions on Power Systems*, vol. 35, no. 4, pp. 2716-2725, Dec. 2019.
[14] M. F. Dynge, P. C del Granado, N. Hashemipour *et al*., "Impact of local electricity markets and peer-to-peer trading on low-voltage grid operations," *Applied Energy*, vol. 301, p. 117404, Nov. 2021.
[15] J. Guerrero, B. Sok, A. C. Chapman *et al*., "Electrical-distance driven peer-to-peer energy trading in a low-voltage network," *Applied Energy*, vol. 287, p. 116598, Apr. 2021.
[16] S. Lilla, C. Orozco, A. Borghetti *et al*., "Day-ahead scheduling of a local energy community: an alternating direction method of multipliers approach," *IEEE Transactions on Power Systems*, vol. 35, no. 2, pp. 1132-1142, Oct. 2019.
[17] C. Orozco, A. Borghetti, B. de Schutter *et al*., "Intra-day scheduling of a local energy community coordinated with day-ahead multistage decisions," *Sustainable Energy*, *Grids and Networks*, vol. 29, p. 100573, Mar. 2022.
[18] J. L. Crespo-Vazquez, T. AlSkaif, Á. M. González-Rueda *et al*., "A community-based energy market design using decentralized decision-making under uncertainty," *IEEE Transactions on Smart Grid*, vol. 12, no. 2, pp. 1782-1793, Nov. 2020.
[19] M. M. Gambini, C. Orozco, A. Borghetti *et al*., "Power loss reduction in the energy resource scheduling of a local energy community," in *Proceedings of 2020 International Conference on Smart Energy Systems and Technologies (SEST)*, Istanbul, Turkey, Sept. 2020, pp. 1-6.
[20] L. Gan, N. Li, U. Topcu *et al*., "Exact convex relaxation of optimal power flow in radial networks," *IEEE Transactions on Automatic Control*, vol. 60, no. 1, pp. 72-87, Jun. 2014.
[21] W. Wei, J. Wang, N. Li *et al*., "Optimal power flow of radial networks and its variations: a sequential convex optimization approach," *IEEE Transactions on Smart Grid*, vol. 8, no. 6, pp. 2974-2987, Mar. 2017.
[22] M. Tofighi-Milani, S. Fattaheian-Dehkordi, M. Fotuhi-Firuzabad *et al*., "Decentralized active power management in multi-agent distribution systems considering congestion issue," *IEEE Transactions on Smart Grid*, vol. 13, no. 5, pp. 3582-3593, May 2022.
[23] L. Wang, Q. Zhou, Z. Xiong *et al*., "Security constrained decentralized peer-to-peer transactive energy trading in distribution systems," *CSEE Journal of Power and Energy Systems*, vol. 8, no. 1, pp. 188-197, Sept. 2021.
[24] T. Morstyn and M. D. McCulloch, "Multiclass energy management for peer-to-peer energy trading driven by prosumer preferences," *IEEE Transactions on Power Systems*, vol. 34, no. 5, pp. 4005-4014, May 2018.
[25] C. Feng, B. Liang, Z. Li *et al*., "Peer-to-peer energy trading under network constraints based on generalized fast dual ascent," *IEEE Transactions on Smart Grid*, vol. 14, no. 2, pp. 1441-1453, Mar. 2023.
[26] H. Sheng, C. Wang, X. Dong *et al*., "Incorporating P2P trading into DSO's decision-making: a DSO-prosumers cooperated scheduling framework for transactive distribution system," *IEEE Transactions on Power Systems*, vol. 38, no. 3, pp. 2362-2375, May 2023.
[27] M. Dolatabadi and P. Siano, "A scalable privacy preserving distributed parallel optimization for a large-scale aggregation of prosumers with residential PV-battery systems," *IEEE Access*, vol. 8, pp. 210950-210960, Nov. 2020.
[28] M. Dolatabadi, P. Siano, and A. Soroudi, "Assessing the scalability and privacy of energy communities by using a large-scale distributed and parallel real-time optimization," *IEEE Access*, vol. 10, pp. 69771-69787, Jun. 2022.
[29] K. Basu, A. Ghoting, R. Mazumder *et al*., "ECLIPSE: an extreme-scale linear program solver for web-applications," in *Proceedings of International Conference on Machine Learning*, virtual conference, Nov. 2020, pp. 704-714.
[30] M. E. Baran and F. F. Wu, "Optimal sizing of capacitors placed on a radial distribution system," *IEEE Transactions on Power Delivery*, vol. 4, no. 1, pp. 735-743, Jan. 1989.
[31] Z. Luo, J. F. Sturm, and S. Zhang. (1996, Jan.). Duality and self-duality for conic convex programming. [Online]. Available: https://repub.eur.nl/pub/1381
[32] D. Goldfarb and K. Scheinberg, "Product-form Cholesky factorization in interior point methods for second-order cone programming," *Mathematical Programming*, vol. 103, no. 1, pp. 153-179, May 2005.
[33] B. O'donoghue, E. Chu, N. Parikh *et al*., "Conic optimization via operator splitting and homogeneous self-dual embedding," *Journal of Optimization Theory and Applications*, vol. 169, no. 3, pp. 1042-1068, Jun. 2016.
[34] S. Cinvalar, J. J. Grainger, H. Yin *et al*., "Distribution feeder reconfiguration for loss reduction," *IEEE Transactions on Power Delivery*, vol. 3, no. 3, pp. 1217-1223, Jul. 1988.
[35] C. Wang and H. Cheng, "Optimization of network configuration in large distribution systems using plant growth simulation algorithm," *IEEE Transactions on Power Systems*, vol. 23, no. 1, pp. 119-126, Jan. 2008.
[36] S. Cui, Y. Wang, Y. Shi *et al*., "An efficient peer-to-peer energy-sharing framework for numerous community prosumers," *IEEE Transactions on Industrial Informatics*, vol. 16, no. 12, pp. 7402-7412, Dec. 2019.
[37] C. Mu, T. Ding, S. Zhu *et al*., "A decentralized market model for a microgrid with carbon emission rights," *IEEE Transactions on Smart Grid*, vol. 14, no. 2, pp. 1388-1402, May 2023.
[38] S. Boyd, S. P. Boyd, and L. Vandenberghe, "Convex optimization," Cambridge: Cambridge University Press, 2004.
[39] N. Halko, P. G. Martinsson, Y. Shkolnisky *et al*., "An algorithm for the principal component analysis of large data sets," *SIAM Journal on Scientific Computing*, vol. 33, no. 5, pp. 2580-2594, Sept. 2011.
[40] A. Beck and M. Teboulle, "A fast iterative shrinkage-thresholding algorithm for linear inverse problems," *SIAM Journal on Imaging Sciences*, vol. 2, no. 1, pp. 183-202, Jan. 2009.
[41] F. Alizadeh and D. Goldfarb, "Second-order cone programming," *Mathematical Programming*, vol. 95, no. 1, pp. 3-51, Jan. 2003.

Mohammad Dolatabadi received the Ph. D. degree in mathematics from Ferdowsi University of Mashhad, Mashhad, Iran, in 2010. Currently, he is an Assistant Professor in the Department of Mathematics, University of Valie-Asr, Rafsanjan, Iran. His research interests include intersection of numerical linear algebra, machine learning and operations, and exploiting matrix theory to large-scale convex optimization for parallel computation while preserving privacy.

Alberto Borghetti graduated (with honors) in electrical engineering at the University of Bologna, Bologna, Italy, in 1992. Since then, he has been working with the power system group of the same university, and is now a Professor of electrical power systems, IEEE Fellow (class 2015). He received the 2016 ICLP Scientific Committee Award and the 2018 CIGRE Technical Council Award. He served as Editor-in-Chief of Electrical Engineering – Archiv fur Elektrotechnik (2019-2023), as an Editor of IEEE Transactions on Smart Grid (2010-2017) and of IEEE Transactions on Power Systems (2018-2022). He is currently serving as an Associate Editor of Journal of Modern Power Systems and Clean Energy. His research and teaching activities are in the areas of power system analysis, power system restoration after blackout, electromagnetic transients, optimal generation scheduling, and distribution system operation.

Pierluigi Siano received the M.Sc. degree in electronic engineering and the Ph. D. degree in information and electrical engineering from the University of Salerno, Salerno, Italy, in 2001 and 2006, respectively. He is a Professor and Scientific Director of the Smart Grids and Smart Cities Laboratory with the Department of Management & Innovation Systems, University of Salerno. He has co-authored more than 680 articles including more than 410 international journals. In 2019-2022, he has been awarded as a Highly Cited Researcher in Engineering by Web of Science Group. He has been the Chair of the IES TC on Smart Grids. He is an Editor for the Power & Energy Society Section of IEEE Access, IEEE Transactions on Power Systems, IEEE Transactions on Industrial Informatics, IEEE Transactions on Industrial Electronics, IEEE Systems. His research interests include demand response, energy management, integration of distributed energy resources in smart grids, electricity markets, and planning and management of power systems.